ISSN 0023-1584, Kinetics and Catalysis, 2011, Vol. 52, No. 1, pp. 48–54. © Pleiades Publishing, Ltd., 2011.

Catalytic Properties of the Cr-HMS Materials in the Benzylation of Benzene with Benzyl Chloride[1]

K. Bachari[a, b], A. Touileb[a], N. Tahir[b], A. Saadi[b], D. Halliche[b], and O. Cherifi[b]

[a]*Centre de Recherche Scientifique et Technique en Analyses Physico-Chimiques (C.R.AP.C) BP 248, Alger RP 16004, Algiers, Algeria*

[b]*Laboratoire de Chimie du Gaz Naturel, Faculté de Chimie, BP 32, 16111 El Alia, U.S.T.H.B., Bab Ezzouar, Algiers, Algeria*

e-mail: bachari2000@yahoo.fr

Received January 8, 2009

Abstract—A series of chromium-containing mesoporous silicas with different Cr contents were prepared and characterized with chemical analysis, N_2 adsorption measurements (BET equation and BJH theory), X-ray diffraction, diffuse reflectance UV–visible and H_2-temperature programmed reduction techniques. Excellent results in benzylation of benzene and substituted benzenes employing benzyl chloride as the alkylating agent were obtained. The mesoporous chromium-containing materials showed both high activity and high selectivity for benzylation of benzene. The activity of these catalysts for the benzylation of different aromatic compounds is in the following order: benzene > toluene > *p*-xylene > anisole. Kinetics of the benzene benzylation over these catalysts has also been investigated.

DOI: 10.1134/S0023158411010022

Chromium-based catalysts have received much attention because of their wide use in many catalytic reactions [1]. Silica- and alumina-supported chromium oxides were industrially used for the production of polyethylene [2, 3] and lower alkenes such as propylene and isobutene through the dehydrogenation of the corresponding alkanes [4, 5], respectively. The redox properties and the appropriate dispersion of chromium species on the support are important in these catalytic reactions [6]. Cr-containing mesoporous molecular sieves (Cr-HMS) were reported to exhibit high photocatalytic reactivity in ethylene polymerization [7]. In the other hand, Friedel–Crafts alkylations comprise a very important class of reactions which are of common use in organic chemistry. These reactions are habitually catalyzed by Lewis acids in liquid phase [8], and the substitution of liquid acids by solid acid catalysts is a challenging task. The alkylation of benzene by benzyl chloride is interesting for the preparation of substituted polychlorobenzenes used as dielectrics. In homogeneous phase this reaction is catalyzed at the industrial scale by $AlCl_3$, $FeCl_3$, BF_3, $ZnCl_2$, and H_2SO_4 [8–10]. The new environmental legislation pushes for the replacement of all liquid acids by solid acid catalysts which are environmentally more friendly catalysts and which lead to minimal pollution and waste [11, 12]. Indeed, several solid acid catalysts have already been proposed which are efficient catalysts such as; Fe-modified ZSM-5 and Hβ zeolites; Fe_2O_3 or $FeCl_3$ deposited on micro-, meso- and macroporous [13]; Fe-containing mesoporous molecular sieves materials [14, 15]; Fe-, Zn-, Ga-, and In-modified ZSM-5 type zeolite catalysts [16]; Ga- and Mg-oxides and chlorides derived from Ga-Mg-hydrotalicite [17]; Ga-SBA-15 [18]; Ga-HMS [19]; $InCl_3$, $GaCl_3$, $FeCl_3$, and $ZnCl_2$ supported on clays and Si-MCM-41 [20]; transition metal chloride supported mesoporous SBA-15 [21]; supported thallium oxide catalysts [22]; Sb supporting K10 [23]; solid superacid and silica-supported polytrifluoromethanesulfosiloxane [24]; Si-MCM-41-supported Ga_2O_3 and In_2O_3 [25]; H_2SO_4, HNO_3, and $HClO_4$/metakaolinite [26]; alkali metal salts and ammonium salts of keggin-type heteropolyacids [27]; ion-exchanged clays [28]; clayzic [29]; Cu-HMS [30]; solid superacids based on sulfated ZrO_2 [31]; HY [32]; Fe, Ce, W-modified Hβ zeolites [33]; H-ZSM-5 [34]; and $FeCl_3$, $MnCl_2$, $CoCl_2$, $NiCl_2$, $CuCl_2$, $ZnCl_2$ supported on acidic alumina [35] for the benzylation of benzene and other aromatic compounds.

In the present work, we report the synthesis and characterization of such materials incorporating chromium and their test as catalysts for the benzylation of benzene with benzyl chloride. The kinetics of the reaction over these catalysts has been investigated and the reaction has been extended to other substrates like toluene, *p*-xylene and anisole.

[1] The article is published in the original.

EXPERIMENTAL

Materials

Samples were synthesized with hexadecylamine (Aldrich), tetraethyl orthosilicate (TEOS, Aldrich), chromium nitrate ($Cr(NO_3)_3$ aqueous solution, Merck) and ethanol (Rhone-Poulenc).

Catalysts Preparation

The catalysts Cr-HMS-*n* (where *n* is the Si/Cr ratio in the precursor gel equal 50, 35, 15, and 5) have been prepared following the pathway reported by Tanev et al. [36]. In a representative preparation, hexadecylamine was added to a solution containing water and ethanol and the mixture was stirred until homogeneous. Then tetraethyl orthosilicate was added under vigorous stirring. The metal precursor (an aqueous solution of $Cr(NO_3)_3$) dissolved in TEOS itself. This solution was then stirred at room temperature for 24 h to obtain the products. The solids were recovered by filtration, washed with distilled water, and air-dried at 393 K. Organic molecules occluded in the mesopores were removed by solvent extraction. The dried precursor was dispersed in ethanol (5 g/100 ml) containing a small amount of NH_4Cl (1 g/100 ml) and the mixture was refluxed under vigorous stirring for 2 h. The solid was then filtered and washed with cold ethanol. The extraction procedure was repeated twice before drying the samples at 393 K in an oven. Finally the samples were calcined at 873 K in air for 4 h.

Characterization of the Samples

The chemical compositions of the samples were determined by a combination of wet chemical methods and atomic absorption spectrometry (Hitachi Z 800). Adsorption–desorption experiments using N_2 were carried out at 77 K on a Nova 2000 porosimeter (Quantachrome) instrument. Before each measurement the samples were first outgassed at 423 K for 12 h at 5×10^{-3} Torr and then at room temperature for 2 h at 3.9×10^{-9} Torr. The N_2 isotherms were used to determine the specific surface areas and pores diameter using the BET (Brunauer–Emmett–Teller) equation and BJH (Barrett–Joyner–Halenda) theory. Powder X-ray diffraction (XRD) patterns were recorded on Siemens D500 diffractometer with CuK_α radiation. They were recorded with 0.02° (2θ) steps and 1 s counting time per step over two angular domains form 1° to 10° (2θ) and from 10° to 80° (2θ). Diffuse reflectance UV–visible (DR UV–vis) spectroscopic measurements were recorded on a UV2100 spectrometer. The spectra were collected at 230–700 nm referenced to $BaSO_4$. H_2-Temperature programmed reduction (H_2-TPR) of catalysts was performed on Chembet3000 chemical adsorption apparatus (Quantachrome) by using a mixture of 5 vol % H_2/Ar as reducing gas with a total flow rate 20 ml/min. A 50 mg sample was heated from room temperature to 700°C at a heating rate of 10°C/min after pre-treatment at 300°C for 30 min in helium gas flow. The reduction signal was recorded by a thermal conductivity detector. The reducing gas was cooled by mixture of *n*-octane and liquid nitrogen to condense the water generated from reduction of the catalyst.

Catalytic Testing

The benzylation reactions over a series of chromium-containing mesoporous silicas catalysts were carried out in a magnetically stirred glass reactor (25 cm^3) fitted with a reflux condenser, having a low dead volume, mercury thermometer and arrangement for continuously bubbling moisture-free nitrogen N_2 (flow rate 30 cm^3 min^{-1} through the liquid reaction mixture, at the following reaction conditions: reaction mixture, containing 15 ml of moisture-free liquid aromatic compound (or 2.5 ml of moisture-free aromatic compound mixed with 12.5 ml of moisture-free solvent), 1.0 ml of benzyl chloride, 0.1 g of catalyst and reaction temperature 353 K. The reaction was started by injecting benzyl chloride in the reaction mixture, containing catalyst and aromatic compound with or without solvent. Measuring quantitatively the HCl evolved in the reaction by acid–base titration (by absorbing the HCl carried by N_2 in a 0.1 M NaOH solution, containing phenolphthalein indicator) followed the course of the reaction. The polybenzyl chlorides (which are formed by the condensation of benzyl chloride) were isolated from the reaction mixture by the procedure given by Choudhary et al. [37]. In all the cases, the major product formed was mainly monobenzylated compound along with polybenzyl chlorides as side products depending upon the condition used. Samples were analyzed periodically on a gas chromatograph HP-6890 equipped with a flame ionization detector and a capillary column RTX-1 (30 m × 0.32 nm i.d.). The products were also identified by GC-MS (HP-5973) analysis.

RESULTS AND DISCUSSION

Characterization

The results of the chemical composition and characteristics of the catalysts are given in the Table 1. The chromium compositions of the solids corresponded relatively well to those fixed for the synthesis except at low chromium content (Cr-HMS-50) where a loss of chromium was observed. Most of the values of the specific surface areas of the solids were larger than 1000 m^2 g^{-1}, which was typical for mesoporous materials. When the chromium content increased, they decreased slightly. The N_2 adsorption isotherms of the samples revealed a uniform pore size. Diffuse reflectance UV–visible spectra of Cr-HMS-*n* with different Si/Cr ratio are shown in Fig. 1. It is generally well

Table 1. Chemical composition and characteristics of the catalysts

Sample	SiO_2/Cr_2O_3 (molar ratio)			Surface area, $m^2 g^{-1}$	ϕ_p, Å*
	gel	chemical analysis	Cr, wt %		
HMS	–	–	–	1170.0	38
Cr-HMS-50	78.0	50	1.8	1143.0	35
Cr-HMS-35	39.0	35	4.2	1114.0	36
Cr-HMS-15	17.2	15	6.9	1085.0	35
Cr-HMS-5	6.4	5	9.1	989.3	34

* ϕ_p is the mean pore diameter obtained from N_2 adsorption isotherms.

known that two bands at 260–280 and 370–380 nm in the charge transfer region are characteristic of the presence of Cr (VI) in tetrahedral coordination, whereas bands at 450–465 and 580–600 nm relate to the $A_{2g} \longrightarrow T_{1g}$ and $A_{2g} \longrightarrow T_{2g}$ transitions of Cr(III) in octahedral symmetry respectively [38, 39]. From Fig. 1, two bands at 260–270 and 360–370 nm appear apparently on Cr-HMS-50 and Cr-HMS-35, indicating the presence of Cr(VI) in tetrahedral coordination. But absorption band at 600 nm characteristic of Cr(III) in octahedral coordination is not detectable on both samples with lower chromium loading. A weak shoulder at 450–470 nm ascribes to Cr(VI) in chromate ions on these two samples. The appearance of band at 600 nm and weakening of bands at 260 and 370 nm demonstrate that part of Cr species form to Cr(III) in octahedral coordination on Cr-HMS-15 and Cr-HMS-5 samples. The O $\longrightarrow$ Cr(III) charge transfer also contributes to absorption bands at 450–465 nm overshadowed that of Cr(VI) chromate. These results reveal that most Cr species form to Cr(VI) in tetrahedral coordination at low chromium loading and the increase of chromium loading causes formation of Cr(III) in octahedral coordination on Cr-HMS-*n* catalysts. Furthermore, the pure siliceous HMS mesoporous molecular sieve gives one broad peak at low angle region corresponding to d_{100} reflection in XRD pattern, indicating the presence of uniform mesoporous channels. Chromium-containing mesoporous silicas Cr-HMS-*n* show one similar XRD peak as pure siliceous HMS mesoporous molecular sieve at about $2\theta = 2°$. Moreover, the intensity of the peak decreased when the chromium content increased showing that the addition of chromium has a negative effect on the crystallinity. At the same time, two weak peaks at $2\theta = 44.5$ and 54.8° corresponding to diffraction of crystal Cr_2O_3 are observed on XRD pattern of Cr-HMS-35. When the chromium content grows (Cr-HMS-15 and Cr-HMS-5), clear diffraction peaks of rhombohedral Cr_2O_3 crystal appear (Fig. 2). In fact, the Cr-HMS-50 does not show any XRD peaks of metal oxide. Indeed, the Cr-HMS-5 shows more intense reflection than

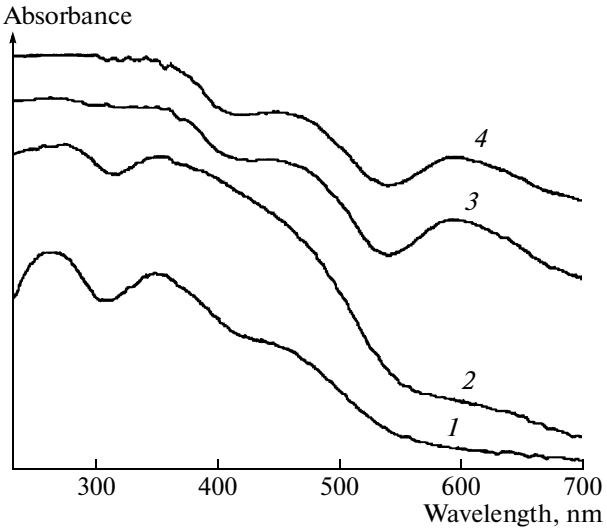

Fig. 1. DR UV–vis spectra of the Cr-HMS-*n* sample: *1*—Cr-HMS-50, *2*—Cr-HMS-35, *3*—Cr-HMS-15, *4*—Cr-HMS-5.

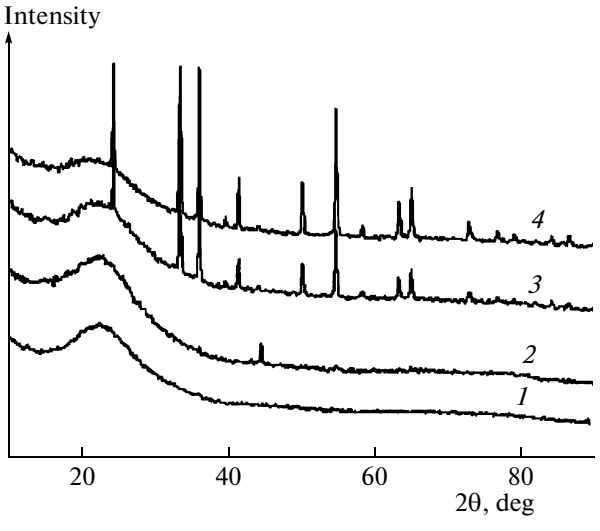

Fig. 2. XRD patterns of the Cr-HMS-*n* catalysts in the domain of 10°–80° (2θ): *1*—Cr-HMS-50, *2*—Cr-HMS-35, *3*—Cr-HMS-15, *4*—Cr-HMS-5.

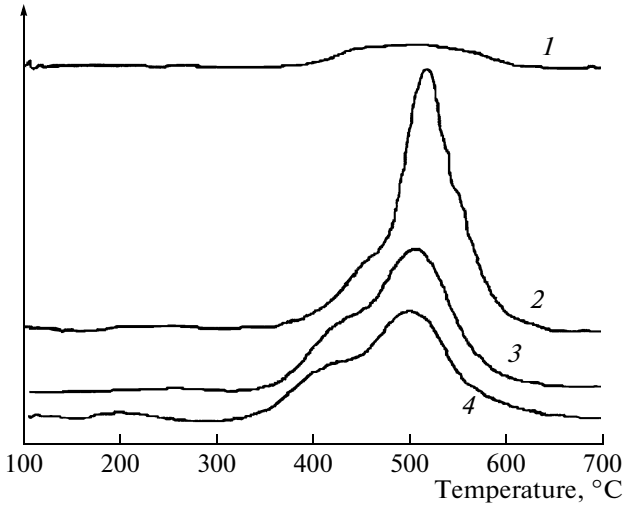

Fig. 3. H_2-TPR patterns of the Cr-HMS-*n* samples: *1*—Cr-HMS-50, *2*—Cr-HMS-35, *3*—Cr-HMS-15, *4*—Cr-HMS-5.

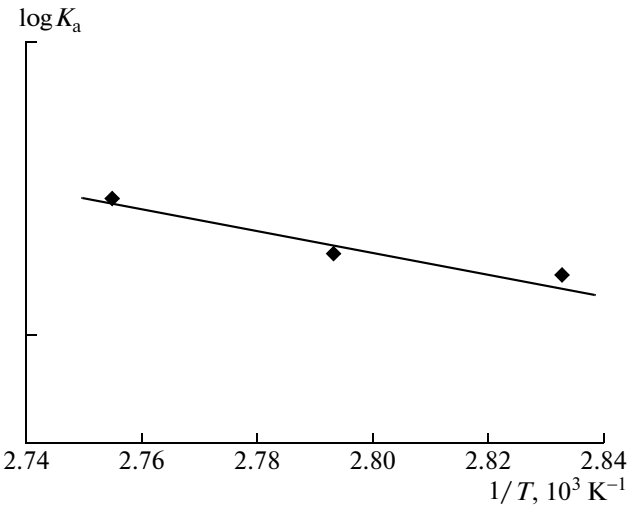

Fig. 4. Arrhenius plot of logK_a as a function of $1/T$ for the benzene benzylation reaction over Cr-HMS-15 catalyst.

Cr-HMS-15. These results correspond to the observation from DR UV–vis that higher content of chromium leads to formation of Cr(III) species on Cr-HMS.

H_2-TPR patterns of Cr-HMS-*n* with different chromium content are shown in Fig. 3. One strong peak at about 500°C with a shoulder at 400–450°C is observed for each sample. These H_2 consumption peaks are assigned to the reduction of Cr(VI) $\longrightarrow$ Cr(III) [39]. Based on the results of Cavani et al. [40], two kinds of Cr(VI) species, the grafted and the soluble Cr(VI), are expected to form on Cr-HMS. The grafted Cr(VI) offers greater interaction with silica support and is harder to be reduced than the soluble Cr(VI), which presents as isolated chromates on the surface of catalyst. Thus, the strong peak at higher temperature corresponds to the reduction of grafted Cr(VI) species and the weak shoulder at lower temperature may result from reduction of soluble Cr (VI).

Reaction Kinetics

The kinetic data for the benzene benzylation reaction in excess of benzene (stoichiometric ratio Bz/BzCl = 15) over the Cr-HMS-15 catalyst could be fitted well to a pseudo-first-order rate law:

$$\log(1/1 - x) = (K_a/2.303)(t - t_0),$$

where K_a is the apparent rate constant, x is the fractional conversion of benzyl chloride, t is the reaction time, and t_0 is the induction period corresponding to the time required for reaching equilibrium temperature. As a function of the time a plot of log $(1/1 - x)$ gives a linear plot over a large range of benzyl chloride conversions. The effect of temperature on the rate was studied by conducting the reaction at 343, 348, and 353 K under the standard reaction conditions (stoichiometric ratio Bz/BzCl = 15 and 0.1 g of catalyst). The results showed that the catalytic performances of the catalyst strongly increased with a growth of the reaction temperature (Table 2). Indeed, the time for 50% conversion of benzyl chloride and the apparent rate constant K_a changed from 337.4 min and 50.4 × 10^{-4} min^{-1} at 343 K to, respectively, 75 min and 132.8 × 10^{-4} min^{-1} at 353 K. By contrast, the selectivity to diphenylmethane decreased from 100 to 70.4%.

Two Bz/BzCl ratios have been investigated. The results obtained are reported on Table 3. It appears that the stoichiometric ratio between benzene and benzyl

Table 2. Catalytic activities of Cr-HMS-15 at 343, 348, and 353 K (Bz/BzCl = 15 and m_{cat} = 0.1 g)

Temperature, K	Time*, min	Selectivity, %		Apparent rate constant K_a, 10^4 min^{-1}
		diphenylmethane	polybenzyl chlorides	
343	337.4	100.0	–	50.4
348	150.0	94.0	6.0	64.5
353	75.0	70.4	29.6	132.8

* Time required for 50% conversion of benzyl chloride.

Table 3. Influence of the stoichiometric ratio Bz/BzCl on selectivity to diphenylmethane at 348 K over Cr-HMS-15 catalyst

Benzene/benzyl cloride ratio	Time*, min	Selectivity, %	
		diphenyl-methane	polybenzyl chlorides
5	437.5	70.2	29.8
15	306.2	100.0	–

* Time required for the complete conversion of benzyl chloride.

chloride has a strong influence on the selectivity to diphenylmethane. With a low ratio, the secondary reactions to dibenzylbenzenes and tribenzylbenzene were favored. Results showing the influence of different substituent groups attached to aromatic benzene nucleus on the conversion of benzyl chloride in the benzylation of corresponding substituted benzenes at 353 K over the Cr-HMS-15 catalyst are presented below.

Reaction rates for substituted benzenes at 353 K over Cr-HMS-15 catalyst (m_{cat} = 0.1 g and substituted benzenes/BzCl = 15)

Substituent	Benzene	Toluene	*p*-Xylene	Anisole
Apparent rate constant K_a, 10^4 min^{-1}	132.8	121.2	114.5	92.5

According to the classical mechanism of the Friedel–Crafts type acid catalyzed benzylation reaction, the benzylation of an aromatic compound is easier if one or more electron donating groups are present in the aromatic ring [8]. Hence, the order for the rate of benzylation for the aromatic compound is expected as follows: anisole > *p*-xylene > toluene ⩾ benzene. But, what is observed in the present case is totally opposite to that expected according to the classical mechanism. The apparent rate constant for the benzylation of benzene and substituted benzenes is in the following order: benzene > toluene > *p*-xylene > anisole. This indicates that, for this catalyst, the reaction mechanism is different from that for the classical acid catalyzed benzylation reactions. On the other hand, the activation energy estimated from the Arrhenius plot is 96 kJ mol^{-1} (Fig. 4). This value is lower than the values recorded for the catalysts In_2O_3/H-ZSM-5 [16] and Ga_2O_3/Hβ [41]. Indeed, it was interesting to compare the solids with Cr-exchanged clays investigated earlier under similar conditions (Bz/BzCl = 15, 353 K) [28]. Both systems reached a final conversion of 100% with complete selectivity to monoalkyl; the half reaction time was about 480 min for Cr/K10 and was here about 75 min, so that Cr-HMS-15 is more active than clays.

Catalytic Performances of Cr-HMS Materials in the Benzylation of Benzene

A comparison of the catalytic properties of the solids tested is presented on Table 4.

The pure mesoporous silica (HMS) and the compounds containing less chromium (Cr-HMS-50 and Cr-HMS-35) were totally inactive. The other compounds showed an activity increasing with their chromium content. However, the selectivity to diphenylmethane at complete conversion of benzyl chloride decreased while the Cr content increased.

Recycling of the Catalysts

The stability of the catalysts has been studied by running the reaction successively with the same catalyst (Cr-HMS-15) under the same conditions without any regeneration between two runs. The reaction was first run under the standard conditions (benzene/benzyl chloride ratio is 15, 353 K) to the complete conversion of benzyl chloride. Then after a period of 8 min another quantity of benzyl chloride was introduced in the reaction mixture leading to the same benzene/benzyl chloride ratio. After the achievement of the second run, the same protocol was repeated a second time. The results, presented in Table 5, showed that the catalyst could be used several times in the ben-

Table 4. Catalytic properties of the catalysts in the benzylation of benzene with benzyl chloride at 348 K (Bz/BzCl = 15 and m_{cat} = 0.1 g)

Catalyst	Time*, min	Selectivity, %		Apparent rate constant K_a, 10^4 min^{-1}
		diphenylmethane	polybenzyl chlorides	
HMS	–	–	–	–
Cr-HMS-50	–	–	–	–
Cr-HMS-35	–	–	–	–
Cr-HMS-15	306.2	100.0	–	64.5
Cr-HMS-5	216.4	90.5	9.5	137.6

* Time required for the complete conversion of benzyl chloride.

Table 5. Effect of recycling of the catalysts in the benzylation of benzene with benzyl chloride at 353 K over Cr-HMS-15 catalyst (Bz/BzCl = 15 and m_{cat} = 0.1 g)

Running	Time*, min	Selectivity, %		Apparent rate constant K_a, 10^4 min^{-1}
		diphenylmethane	polybenzyl chlorides	
Fresh	427.1	80.6	19.4	132.8
First run	447.3	81.5	18.5	129.5
Second run	459.8	79.3	20.7	130.7

* Time required for the complete conversion of benzyl chloride.

zene benzylation process without a significant change of its catalytic activity.

In conclusion, mesoporous catalysts Cr-HMS-*n* were synthesized with different Cr content and exhibited excellent activities in the benzylation of benzene and substituted benzenes reaction. XRD, DR UV–vis and H_2-TPR characterizations demonstrate that chromium content in Cr-HMS-*n* has significant effect on oxidation state and coordination of chromium species. Cr (VI) species corresponding to chromate form the main local structure of chromium at low Cr content. The percentage of Cr (VI) decrease and crystal Cr_2O_3 appear with an increase of Cr loading. Two kinds of Cr (VI) with different reduced abilities are differentiated by H_2-TPR method. Furthermore, the mechanism involves probably a redox step at the reaction initiation. This gives a greater independence to the effect of substituents, and shows a low sensitivity to water.

REFERENCES

1. Weckhuysen, B.M., Wachs, I.E., and Schoonheydt, R.A., *Chem. Rev.*, 1996, vol. 96, p. 3327.
2. MacDaniel, M., *Adv. Catal.*, 1985, vol. 33, p. 47.
3. Pullukat, T.J. and Hoff, R.E., *Catal. Rev. Sci. Eng.*, 1999, vol. 41, p. 389.
4. Mentasty, L.R., Gorriz, O.F., and Cadus, L.E., *Ind. Eng. Chem. Res.*, 1999, vol. 38, p. 396.
5. Hakuli, A., Harlin, M.E., Backman, L.B., and Krause A.O.I., *J. Catal.*, 1999, vol. 184, p. 349.
6. Cherian, M., Rao, M.S., Hirt, A.M., Waches, I.E., and Deo, G., *J. Catal.*, 2002, vol. 211, p. 482.
7. Yamashita, H., Yoshizawa, K., Ariyuli, M., Higashimoto, S., and Anpo, M., *Stud. Surf. Sci. Catal.*, 2002, vol. 141, p. 495.
8. Olah, G.A., *Friedel–Crafts Chemistry*, New York: Wiley-Interscience, 1973.
9. Olah, G.A., Prakash, G.K.S.J., and Sommer, J., *Superacids*, New York: Wiley-Interscience, 1985.
10. Commandeur, R., Berger, N., Jay, P., and Kervenal, J., Eur. Patent 0422986, 1991.
11. Clark, J.H., Cullen, S.R., Barlow, S.J., and Bastock, T.W., *J. Chem. Soc., Perkin Trans. 2*, 1994, no. 6, p. 1117.
12. Cao, J., He, N., Li, C., Dong, J., and Xu, Q., *Mesoporous Mol. Sieves*, 1998, vol. 117, p. 461.
13. Choudhary, V.R., Jana, S.K., and Mamman, A.S., *Microporous Mesoporous Mater.*, 2002, vol. 56, p. 65.
14. He, N., Bao, S., and Xu, Q., *Appl. Catal., A*, 1998, vol. 169, p. 29.
15. Bachari, K., Millet, J.M.M., Benaichouba, B., Cherifi, O., and Figueras, F., *J. Catal.*, 2004, vol. 221, p. 55.
16. Choudhary, V.R. and Jana, S.K., *Appl. Catal., A*, 2002, vol. 224, p. 51.
17. Choudhary, V.R., Jana, S.K., and Narkhede, V.S., *Appl. Catal., A*, 2002, vol. 235, p. 207.
18. El Berrichi, Z., Cherif, L., Orsen, O., Fraissard, J., Tessonnier, J.P., Vanhaecke, E., Louis, B., Ledoux, M.J., and Pham-Huu, C., *Appl. Catal., A*, 2006, vol. 298, p. 194.
19. Bachari, K. and Cherifi, O., *J. Mol. Catal. A: Chem.*, 2006, vol. 253, p. 187.
20. Choudhary, V.R. and Jana, S.K., *J. Mol. Catal. A: Chem.*, 2002, vol. 180, p. 267.
21. Bachari, K. and Cherifi, O., *J. Mol. Catal. A: Chem.*, 2006, vol. 260, p. 19.
22. Choudhary, V.R. and Jana, S.K., *J. Catal.*, 2001, vol. 201, p. 225.
23. Deshpande, A.B., Bajpai, A.R., and Samant, S.D., *Appl. Catal., A*, 2001, vol. 209, p. 229.
24. Zhou, D.-Q., Yang, J.-H., Dong, G.-M., Huang, M.-Y., and Jiang, Y.-Y., *J. Mol. Catal. A: Chem.*, 2000, vol. 159, p. 85.
25. Choudhary, V.R., Jana, S.K., and Kiran, B.P., *J. Catal.*, 2000, vol. 192, p. 257.
26. Sabu, K.R., Sukumar, R., Rekha, R., and Lalithambika, M., *Catal. Today*, 1999, vol. 49, p. 321.
27. Izumi, Y., Ogawa, M., and Urabe, K., *Appl. Catal., A*, 1995, vol. 132, p. 127.
28. Cseri, T., Bekassy, S., Rizner, S., and Figueras, F., *J. Mol. Catal. A: Chem.*, 1995, vol. 98, p. 101.
29. Barlow, S.J., Bastock, T.W., Clark, J.H., and Cullen, S.R., *Tetrahedron Lett.*, 1993, vol. 34, no. 20, p. 3339.
30. Bachari, K. and Cherifi, O., *Catal. Commun.*, 2006, vol. 7, p. 926.
31. Koyande, S.N., Jaiswal, R.G., and Jayaram, R.V., *Ind. Eng. Chem. Res.*, 1998, vol. 37, p. 908.

32. Cog, B., Gourves, V., and Figueras, F., *Appl. Catal., A*, 1993, vol. 100, p. 69.

33. Narender, N., Krishna Mohan, K.V.V., Kulkarni, S.J., and Ajit Kumar Reddy, I., *Catal. Commun.*, 2006, vol. 7, p. 583.

34. Choudhary, V.R., Jana, S.K., and Kiran, B.P., *Catal. Lett.*, 1999, vol. 59, p. 217.

35. Salavati-Niasari, M., Hasanalian, J., and Najafian, H., *J. Mol. Catal. A: Chem.,* 2004, vol. 209, p. 209.

36. Tanev, P.T., Chibwe, M., and Pinnavaia, T.J., *Nature*, 1994, vol. 368, p. 317.

37. Choudhary, V.R., Jana, S.K., and Kiran, B.P., *Catal. Lett.*, 2000, vol. 64, p. 223.

38. Rossi, S.D., Casaletto, M.P., Ferraris, G., Cimino. A., and Minelli, G., *Appl. Catal., A*, 1998, vol. 167, p. 257.

39. Gaspar, A.B., Brito, J.L.F., and Dieguez, L.C., *J. Mol. Catal. A: Chem.*, 2003, vol. 203, p. 251.

40. Cavani, F., Koutyrev, M., Trifiro, F., Bartolini, A., Ghisletti, D., Iezzi, R., Santucci, A., and Del Piero, G., *J. Catal.*, 1996, vol. 158, p. 236.

41. Choudhary, V.R., Jana, S.K., Patil, N.S., and Bhargava, S.K., *Microporous Mesoporoua Mater.*, 2003, vol. 57, p. 21.